Optimal Plant Shaping for High Bandwidth Disturbance Rejection in Discrete Disturbance Observers

Xu Chen and Masayoshi Tomizuka

Abstract— **The Q-filter cut-off frequency in a Disturbance Observer (DOB) is restricted by the model mismatch between the plant and its nominal model. DOB Robustness is usually poor when the cut-off frequency of Q-filter increases. In this paper, robustness of the DOB is improved by shaping the true plant with a cascaded frequency shaping filter, while the nominal plant model remains fixed. Once the shaping filter is optimally designed based on DOB robust stability, the cut-off frequency of Q-filter can be greatly increased without loss of stability. The proposed algorithm is implemented on a typical tracking problem, i.e., the spiral writing in hard disk drives.**

I. INTRODUCTION

Fast and accurate tracking control under the presence of disturbances is a central problem in mechanical positioning systems. High bandwidth and high robustness are two main objectives in the control of these devices. One effective way for disturbance attenuation is to use a disturbance observer (DOB), which estimates the disturbance and feeds the negative of the estimated signal back to the plant input to accomplish the disturbance rejection. Examples of successful DOB applications include hard disk drives [1]–[3], optical disk drives [4], linear motors [5], [6], and positioning tables [7].

A standard DOB dynamically links together the actual plant, the inverse of a nominal plant model and the so-called Q-filter, which is normally a low-pass filter. The cut-off frequency, ω_c, of the Q-filter plays an essential role in DOB performance and robustness. From the command following point of view, the DOB loop approximates the nominal plant model below the Q-filter's cut-off frequency, and approximates the true plant when the magnitude of Q-filter drops to a small value. From the disturbance rejection point of view, the higher the cut-off frequency ω_c, the larger the disturbance rejection capacity. However, robustness also decreases as ω_c increases. Therefore, the cut-off frequency of Q-filter is usually restricted to maintain the system robustness. A typical example of this trade-off can be found in [3].

For a robust motion control system, DOB, feedback and feed-forward control strategies are usually combined. In such a case, DOB is applied as an inner loop robust compensator to attenuate the low frequency disturbance and to provide the required robust performance of the feed-forward controller. An effective feed-forward controller requires an accurate model within an as large frequency region as possible, which in turn translates to the requirement of a higher Q-filter cut-off frequency. Increasing the disturbance rejection capacity while maintaining the robust stability is thus a key point to achieve high performance tracking.

There have been many attempts to address the DOB robustness problem. The existing investigations have mainly been rooted in the designs of the Q-filter [8], [9] and the outer loop controllers [10]. In this paper, the robustness improvement of DOB is considered from another aspect. It is proposed to modify the dynamics on the side of the true plant. The robustness of DOB is improved by shaping the true plant with a cascaded filter, while the nominal plant model remains fixed. Once an optimal shaping filter is designed that minimizes the model uncertainties, the cut-off frequency of Q-filter can be greatly increased without loss of stability.

The remainder of this paper is organized as follows. Section II provides a review of the standard digital disturbance observer. The proposed DOB based on optimal plant shaping algorithm is presented in Section III. The efficacy of the proposed method is shown in Section IV, along with a typical tracking problem in hard disk drive systems. Section V concludes the paper.

II. REVIEW OF THE STANDARD DISCRETE DOB

Discrete DOB will be reviewed here briefly. Further discussions can be found in [7], [11], [12].

A. Standard Discrete DOB Structure

Consider a plant $G_p(s)$, with a zero order holder equivalence $G_p(z^{-1})$, and a low-order nominal model[1] $G_n(z^{-1}) = z^{-m}G_{ni}(z^{-1})$. A standard digital DOB can be constructed as shown in Fig. 1(a), where $Q(z^{-1})$ is the low-pass Q-filter, $G_{ni}(z^{-1})^{-1}$ is the inverse of the nominal plant without delays, $u(k)$, $w(k)$, $y(k)$, and $n(k)$ are the control input, the plant input disturbance, the plant output, and the measurement noise. A stable inverse model $G_{ni}(z^{-1})^{-1}$ is needed in the above DOB design. If $G_{ni}(z^{-1})$ has minimal phase, its inverse can directly be assigned, if not, stable inversion techniques

Xu Chen is with the Mechanical Systems Control Laboratory, Department of Mechanical Engineering, University of California, Berkeley, CA, 94720, USA maxchen@me.berkeley.edu

Masayoshi Tomizuka is with the Faculty in the Department of Mechanical Engineering, University of California, Berkeley, CA, 94720, USA tomizuka@me.berkeley.edu

[1]For the DOB design, we intentionally factorize out the delay terms z^{-m}. $G_{ni}(z^{-1})$ is the factorized nominal plant for DOB inverse.

such as the ZPET method [13] should be applied. Figure 1(a) can be transformed to an equivalent form as shown in Fig. 1(b). It is straightforward to derive the following transfer functions from $u^*(k)$, $n(k)$, and $w(k)$ to the output $y(k)$:

$$G_{u^*y}\left(z^{-1}\right)=\frac{G_p\left(z^{-1}\right)G_{ni}\left(z^{-1}\right)}{G_{ni}\left(z^{-1}\right)+\left(G_p\left(z^{-1}\right)-G_{ni}\left(z^{-1}\right)z^{-m}\right)Q\left(z^{-1}\right)} \quad (1)$$

$$G_{ny}\left(z^{-1}\right)=\frac{-G_p\left(z^{-1}\right)Q\left(z^{-1}\right)}{G_{ni}\left(z^{-1}\right)+\left(G_p\left(z^{-1}\right)-G_{ni}\left(z^{-1}\right)z^{-m}\right)Q\left(z^{-1}\right)} \quad (2)$$

$$G_{wy}\left(z^{-1}\right)=\frac{G_p\left(z^{-1}\right)G_{ni}\left(z^{-1}\right)\left(1-Q\left(z^{-1}\right)z^{-m}\right)}{G_{ni}\left(z^{-1}\right)+\left(G_p\left(z^{-1}\right)-G_{ni}\left(z^{-1}\right)z^{-m}\right)Q\left(z^{-1}\right)} \quad (3)$$

The output $y(k)$ can thus be expressed as:

$$y(k)=G_{u^*y}\left(z^{-1}\right)u^*(k)+G_{wy}\left(z^{-1}\right)w(k)+G_{ny}\left(z^{-1}\right)n(k). \quad (4)$$

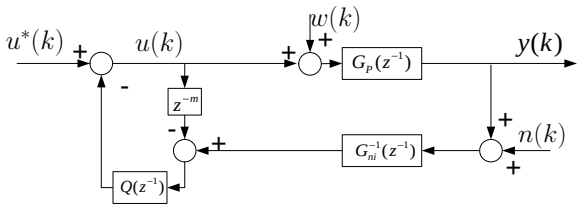

(a) Standard form

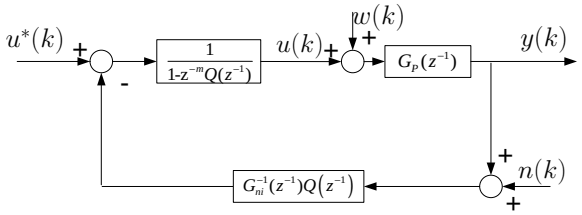

(b) Equivalent form

Fig. 1. Block diagram of the standard digital DOB.

In the low frequency region where $Q(z^{-1})\approx 1$, if the delay is small so that $(1-z^{-m})G_{ni}\approx 0$, then $G_{wy}(z^{-1})\approx 0$ in (3), $G_{ny}(z^{-1})\approx -1$ in (2), and $G_{u^*y}(z^{-1})\approx G_n$ in (1). The disturbance $w(k)$ is thus attenuated and the entire DOB loop behaves like the nominal plant $G_n(z^{-1})$. This observation makes it possible to design other feedback or feed-forward controllers simply based on the low order nominal model. In the high frequency region where $Q(z^{-1})\approx 0$, DOB is essentially inactive, therefore $G_{u^*y}(z^{-1})\approx G_p(z^{-1})$, $G_{wy}(z^{-1})\approx G_p(z^{-1})$, and $G_{ny}(z^{-1})\approx 0$, which indicates that the high frequency sensor noise is attenuated.

B. Stability Robustness

When there are unmodeled dynamics in the plant, the cut-off frequency of the Q-filter should be carefully selected. Consider $G_p(z^{-1})$ as a perturbed version of the nominal model $z^{-m}G_{ni}(z^{-1})$, and the unmodeled dynamics as a multiplicative perturbation $\Delta(z^{-1})$,

$$G_p\left(z^{-1}\right)=z^{-m}G_{ni}\left(z^{-1}\right)\left(1+\Delta\left(z^{-1}\right)\right). \quad (5)$$

From (1), the closed loop characteristic polynomial is given by

$$A_c\left(z^{-1}\right)=G_{ni}\left(z^{-1}\right)+\left(G_p\left(z^{-1}\right)-G_{ni}\left(z^{-1}\right)z^{-m}\right)Q\left(z^{-1}\right) \quad (6)$$

Substituting (5) to (6), we have

$$A_c\left(z^{-1}\right)=G_n\left(z^{-1}\right)\left(z^m+\Delta\left(z^{-1}\right)Q\left(z^{-1}\right)\right). \quad (7)$$

From (7), a sufficient condition for DOB to be stable is that the zeros of $G_n(z^{-1})$ are all in the unit circle and that

$$\left|\Delta\left(e^{j\omega}\right)Q\left(e^{j\omega}\right)\right|<1 \quad \forall\omega. \quad (8)$$

Selection of the nominal plant model has been discussed at the beginning of this subsection. The difficulty for maintaining stability is mainly caused by the unmodeled dynamics $\Delta(z^{-1})$, as we observe in the following section.

III. DOB BASED ON OPTIMAL PLANT SHAPING

In practice, many mechanical systems have good models in the mid-low frequency range and fixed high frequency resonance modes. Examples of such systems include but not limited to servo track writers [14], optical disk drives [4], hard disk drives [15], and direct-drive positioning tables [7]. The major resonance modes usually can be well modeled as second order damping systems with transfer functions $k_i/\left(s^2+2\times\zeta_i'\omega_i s+\omega_i^2\right)$. For example, in Hard Disk Drives (HDDs), the Voice Coil Motor (VCM) actuator system [16] typically has a frequency response as shown in the solid line in Fig. 2.

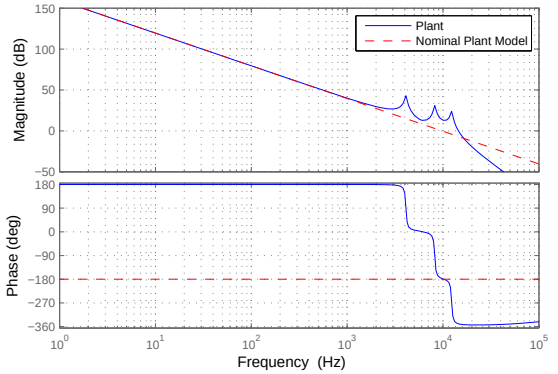

Fig. 2. Frequency responses of a VCM actuator system and the nominal plant model.

When DOB is applied to systems having resonances as discussed above, the nominal model is usually selected ignoring the resonance modes, to achieve a stable inverse nominal model $G_{ni}(z^{-1})^{-1}$, and to simplify the design of feedback or feed-forward controllers outside

the DOB loop. It is desired that sensors for output measurement are accurate, such that sensor noise contributes little to the output error. Under such conditions, it may be preferred that the cut-off frequency of Q-filter be chosen as high as possible. However, according to the DOB stability condition in (8), the ignored resonance modes will severely limit the bandwidth of Q-filter and thus the disturbance rejection capacity of DOB. Figure 3 shows the Q-filter designed in a standard DOB where the plant is the VCM actuator system in Fig. 2, sampled at 2.64 kHz. It is seen that in order to maintain the DOB stability, the Q-filter's cut-off frequency ω_c is limited to be below 320 Hz. To achieve a larger ω_c, we hereby propose a new modified disturbance observer structure by shaping the plant to minimize the modeling error.

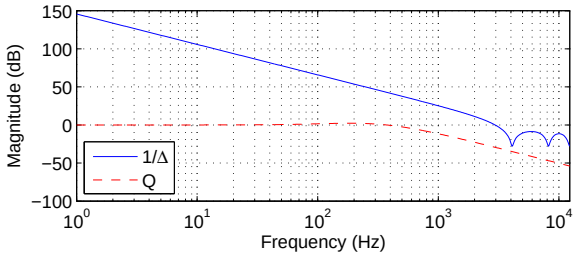

Fig. 3. Magnitude responses of $Q(z^{-1})$ and $1/\Delta(z^{-1})$ in the standard DOB: cut-off frequency of Q-filter restricted to be below 320 Hz.

A. Controller Structure and Properties

Figure 4 shows the structure of the proposed DOB. Different from the standard form, a shaping filter $G_s\left(z^{-1}\right)$ is cascaded preceding the plant $G_p\left(z^{-1}\right)$. Defining the shaped plant $\bar{G}_p\left(z^{-1}\right) := G_p\left(z^{-1}\right)G_s\left(z^{-1}\right)$, we now have

$$\begin{aligned} G_{u^*y}\left(z^{-1}\right) &= \frac{\bar{G}_p\left(z^{-1}\right)G_{ni}\left(z^{-1}\right)}{G_{ni}\left(z^{-1}\right)+\left[\bar{G}_p\left(z^{-1}\right)-G_n\left(z^{-1}\right)\right]Q\left(z^{-1}\right)}, \\ G_{ny}(z^{-1}) &= \frac{-\bar{G}_p\left(z^{-1}\right)Q\left(z^{-1}\right)}{G_{ni}\left(z^{-1}\right)+\left[\bar{G}_p\left(z^{-1}\right)-G_n\left(z^{-1}\right)\right]Q\left(z^{-1}\right)}, \\ G_{wy}(z^{-1}) &= \frac{G_p\left(z^{-1}\right)G_{ni}\left(z^{-1}\right)\left[1-Q\left(z^{-1}\right)z^{-m}\right]}{G_{ni}\left(z^{-1}\right)+\left[\bar{G}_p\left(z^{-1}\right)-G_n\left(z^{-1}\right)\right]Q\left(z^{-1}\right)}. \end{aligned} \quad (9)$$

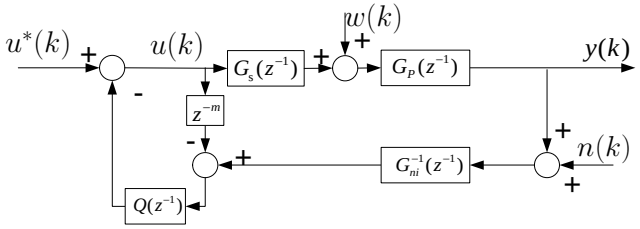

Fig. 4. Block diagram: DOB based on optimal plant shaping.

TABLE I
PROPERTIES OF THE PROPOSED DOB WHEN $z^{-m} \approx 1$.

Q-filter	$Q\left(z^{-1}\right) \approx 1$	$Q\left(z^{-1}\right) \approx 0$
$G_{u^*y}\left(z^{-1}\right)$	$G_{u^*y}\left(z^{-1}\right) \approx G_n\left(z^{-1}\right)$	$G_{u^*y}\left(z^{-1}\right) \approx \bar{G}_p\left(z^{-1}\right)$
$G_{wy}\left(z^{-1}\right)$	$G_{wy}\left(z^{-1}\right) \approx 0$	$G_{wy}\left(z^{-1}\right) \approx G_p\left(z^{-1}\right)$
$G_{ny}\left(z^{-1}\right)$	$G_{ny}\left(z^{-1}\right) \approx -1$	$G_{ny}\left(z^{-1}\right) \approx 0$

Parallel to the analysis in Section II, Table I can be constructed. It is seen that the modified DOB possesses all the advantages of a standard DOB, i.e., low frequency disturbance rejection, nominal model following, and high frequency sensor noise attenuation. Moreover, superior to the standard disturbance observer, the modified DOB has the following additional properties:

1) Resonance attenuation: from Table I, in the high frequency region, the DOB loop behaves like $G_{u^*y}(z^{-1}) \approx \bar{G}_p(z^{-1}) = G_p(z^{-1})G_s(z^{-1})$. If a shaping filter is properly constructed, the resonance modes can then be well attenuated.
2) Enlarged disturbance rejection bandwidth: by careful design, $G_s(z^{-1})$ can actively reduce the mismatch between $\bar{G}_p(z^{-1})$ and $G_n(z^{-1})$. After optimization of $G_s(z^{-1})$, the cut-off frequency of $Q(z^{-1})$, and thus the DOB disturbance rejection bandwidth, can be greatly enlarged.

B. Stability Robustness

Similar to Section II, we have the following results for the proposed DOB structure:

The closed loop characteristic polynomial:

$$\bar{A}_c\left(z^{-1}\right) = G_{ni}\left(z^{-1}\right) + \left[\bar{G}_p\left(z^{-1}\right) - G_n\left(z^{-1}\right)\right]Q\left(z^{-1}\right). \quad (10)$$

Let $\bar{G}_p\left(z^{-1}\right)$ be subjected to multiplicative model uncertainties:

$$\bar{G}_p\left(z^{-1}\right) = G_n\left(z^{-1}\right)\left(1+\bar{\Delta}\left(z^{-1}\right)\right), \quad (11)$$

where

$$\bar{\Delta}\left(z^{-1}\right) = \frac{G_p\left(z^{-1}\right)G_s\left(z^{-1}\right) - G_n\left(z^{-1}\right)}{G_n\left(z^{-1}\right)}. \quad (12)$$

The stability of the modified DOB requires $G_n\left(z^{-1}\right)$ to have no zeros outside the unit circle and that

$$\left|\bar{\Delta}\left(e^{j\omega}\right)Q\left(e^{j\omega}\right)\right| < 1 \quad \forall\omega. \quad (13)$$

Equation (13) appears to have a similar structure with (8), except that here $\bar{\Delta}(z^{-1})$ is the multiplicative model uncertainty between $\bar{G}_p(z^{-1})$ and $G_n(z^{-1})$, while in the standard DOB $\Delta\left(z^{-1}\right) = \left[G_p\left(z^{-1}\right) - G_n\left(z^{-1}\right)\right]/G_n\left(z^{-1}\right)$. Assuming that the nominal plant model remains the same in the two cases, in the proposed DOB, by cascading the shaping filter to the plant, we make the magnitude of $\bar{\Delta}(e^{j\omega})$, and thus that of $\left|\bar{\Delta}\left(e^{j\omega}\right)Q\left(e^{j\omega}\right)\right|$ smaller. Therefore, the Q-filter can have a higher cut-off frequency in the proposed method.

C. Shaping Filter Design

Define x as the coefficient vector to be optimized in the shaping filter. Based on the previous discussion, x should be chosen such that:

$$J(x) = \left\| G_s(x, e^{j\omega}) G_p(e^{j\omega}) - G_n(e^{j\omega}) \right\|_2^2 \tag{14}$$

is minimized over the frequency range where there is strong model mismatch between $G_p(z^{-1})$ and $G_n(z^{-1})$. For the plant in Fig. 2, direct inspection gives that the range [1 kHz, 13 kHz] needs to be taken into the optimization.

Notice that (14) contains two optimization problems, the magnitude matching to minimize $\left\| |G_s(e^{j\omega}) G_p(e^{j\omega})| - |G_n(e^{j\omega})| \right\|_2^2$, and the phase matching to minimize $\left\| \text{phase}\left(G_s(e^{j\omega}) G_p(e^{j\omega})\right) - \text{phase}\left(G_n(e^{j\omega})\right) \right\|_2^2$.

For the magnitude matching, when resonances are the main sources of model mismatch, the structure of the shaping filter can be a combination of several notch filters, i.e.,

$$G_s(s) = \prod_{i=1}^{m} \frac{s^2 + 2\zeta_i \bar{\omega}_i s + \bar{\omega}_i^2}{s^2 + 2x_i \bar{\omega}_i s + \bar{\omega}_i^2}, \tag{15}$$

where ζ_i and $\bar{\omega}_i$ are the damping ratio and center frequency of the i^{th} resonance, and are obtained through system identification. x_i ($x_i > \zeta_i$ for notch filters) is the notch coefficient that needs tuning. It is easier to perform optimization in the continuous time domain, by noting that the magnitude response at frequency ω_k is given by

$$|G_s(j\omega_k)| = \prod_{i=1}^{m} \frac{\sqrt{\left(\bar{\omega}_i^2 - \omega_k^2\right)^2 + 4\bar{\omega}_i^2 \omega_k^2 \zeta_i^2}}{\sqrt{\left(\bar{\omega}_i^2 - \omega_k^2\right)^2 + 4\bar{\omega}_i^2 \omega_k^2 x_i^2}}. \tag{16}$$

Taking the log to normalize the unit to dB, we have

$$f_k(y) = 20\log|G_s(j\omega_k)| = M_k - 10\sum_{i=1}^{m} \log\{A_k + B_k y_i\}, \tag{17}$$

where $y_i = x_i^2$, $A_k = \left(\bar{\omega}_i^2 - \omega_k^2\right)^2$, $B_k = 4\bar{\omega}_i^2 \omega_k^2$, and $M_k = 10\sum_{i=1}^{m} \log\left\{A_k + B_k a_i^2\right\}$. Noting that $\log|G_s(j\omega) G_p(j\omega)| = \log|G_s(j\omega)| + \log|G_p(j\omega)|$, we transform the magnitude matching in (14) to the following simplified version:

$$\min_{y \in \mathbb{R}^m} \left\| f(y) - 20\left(\log|G_n(j\omega)| - \log|G_p(j\omega)|\right) \right\|_2^2 \tag{18}$$

$$\text{subject to } \zeta_i^2 < y_i < 1,\ i = 1, 2, \ldots, m \tag{19}$$

where $f(y)$, $\log|G_n(j\omega)|$, and $\log|G_p(j\omega)|$ are column vectors with each of their elements being the magnitude response at selected frequency points. This is a nonlinear least squares problem. When the number of parameters to be identified is small, performing direct line search to y_i over the region $[\zeta_i^2, 1]$, i.e., evaluating the objective function at a variety of parameter values in the input space, can lead us to the minimal. Otherwise, nonlinear programming based on combined gradient and Newton methods can be applied. The latter can be performed in MATLAB using the nonlinear least squares data fitting function *lsqcurvefit*.

The $G_s(s)$ derived above is then digitized to $G_s(z^{-1})$, using MATLAB's *c2d* function with the pole zero match method (*matched*). The phase match problem can now be addressed by adding delay z^{-j} or advance elements z^j into $G_s(z^{-1})$, and examining directly the phase difference between $G_s(e^{j\omega}) G_p(e^{j\omega})$ and $G_n(e^{j\omega})$ in the frequency response. For causality, when z^j is needed, instead of modifying $G_s(z^{-1})$, z^{-j} can be added to $G_n(z^{-1})$, since minimizing the phase difference between $z^j G_s(z^{-1}) G_p(z^{-1})$ and $G_n\left(z^{-1}\right)$ is equivalent to minimizing the phase difference between $G_s(z^{-1}) G_p(z^{-1})$ and $z^{-j} G_n\left(z^{-1}\right)$. However, to achieve a DOB with high performance, the delay elements should not be too many [11].

IV. CASE STUDY

The proposed algorithm is implemented in a typical tracking problem, the spiral writing in hard disk drives. The spiral writing task is performed on a servo track writer, which uses the VCM actuator system for positioning. The servo writer head is expected to follow a reference trajectory as shown in Fig. 5 when moving from the disk outer diameter to the inner diameter. The goal is to achieve constant velocity as soon as possible with smooth settling and minimum tracking error.

The well formulated open-source HDD benchmark tool in [16] was used in simulations. The plant has a frequency response as shown in Fig. 2. The disturbances include the torque disturbance, disk fluttering, the repeatable runout, and the measurement noise. The system has a sampling time of 3.788×10^{-5} sec.

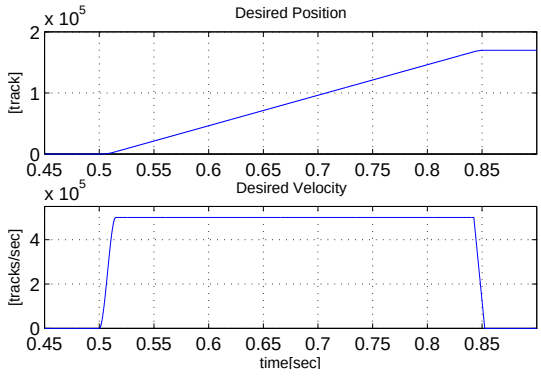

Fig. 5. Reference trajectory for spiral writing: the actuator starts acceleration at 0.5sec, quickly reaches a constant speed for spiral writing, and finally decelerates to zero speed.

The Q-filter used in this paper is given by

$$Q(s) = \frac{3\tau s + 1}{(\tau s + 1)^3}, \tag{20}$$

where τ is a time parameter that determines the cut-off frequency. It has been suggested in [12] that such a Q-filter results in balanced low frequency and high frequency performances. The Q-filter was digitalized using bilinear transformation for implementation.

The solid line and the dotted line in Fig. 6 show the frequency responses of the plant and the nominal plant. There are three dominant resonant modes in the plant. The shaping filter is the product of three notch filters. In the magnitude matching, the notch coefficients were all initialized at 0.1, and converged to the optima $[0.403,\ 0.316,\ 0.364]^T$.

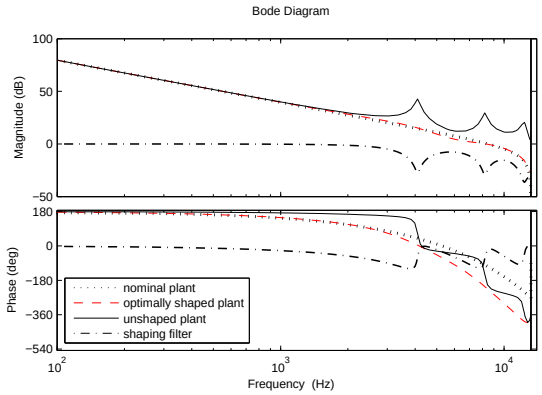

Fig. 6. Frequency responses of the plant, optimally shaped plant, the shaping filter, and the nominal plant.

Figure 7 shows graphically the robust stability conditions in the proposed DOB structure. Compared with Fig. 3, the high frequency model uncertainties have been greatly reduced, and the Q-filter cut-off frequency can now increase from 320 Hz to as large as 2000 Hz.

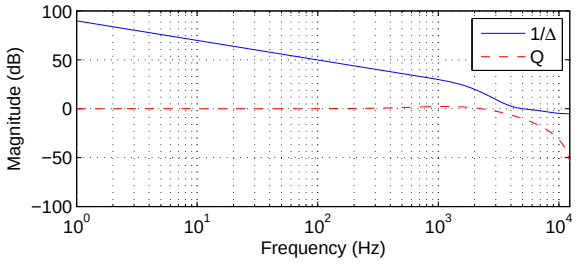

Fig. 7. Magnitude responses of $Q(z^{-1})$ and $1/\Delta(z^{-1})$ in the proposed DOB: Q-filter cut-off frequency can expand to as large as 2000 Hz.

The shaping filter brought some phase drop starting at around 1kHz. Phase matching was thus performed after the magnitude matching. Note that digital disturbance observers accept only integer amounts of delays. Two delay steps were added to achieve the good phase match up to about 3 kHz, which is high enough for normal servo operation. The nominal plant finally developed a form as a double integrator with two delay steps.

The overall controller structure is shown in Fig. 8. The proposed DOB was applied as an inner loop controller. The DOB loop was then stabilized by a PD type feedback controller $G_{PD}(z^{-1})$, to meet the stability and the bandwidth requirements. The disturbance observer makes the DOB loop behave like the nominal plant $G_n(z^{-1})$, and remain robust in the presence of low frequency disturbances. Therefore, below the cut-off frequency of $Q(z^{-1})$, the feedback closed loop transfer function will be close to

$$G_{closed}(z^{-1}) = \frac{G_n(z^{-1})G_{PD}(z^{-1})}{1+G_n(z^{-1})G_{PD}(z^{-1})}. \tag{21}$$

Finally, a feed-forward zero phase error tracking [13] controller $G_{ZPET}(z^{-1})$ was constructed based on $G_{closed}(z^{-1})$, to achieve high performance tracking.

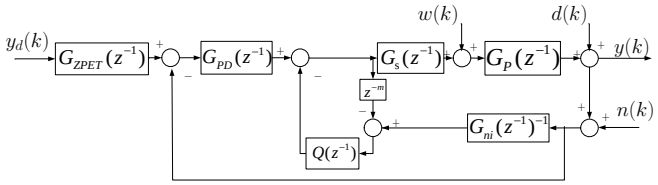

Fig. 8. Overall controller structure applying the DOB based on optimal plant shaping. $w(k)$, $d(k)$, and $n(k)$ are respectively the input disturbance, the output disturbance, and the sensor noise.

For comparison, another simulation was performed with the proposed DOB replaced by the standard DOB[2]. Figure 9 shows tracking errors of the system in the two cases. The maximum error dropped from 0.21 track pitch (TP) in the standard DOB to 0.13 TP in the proposed DOB, implying a 38% improvement. The standard deviation of the error decreased from 0.0518 to 0.0319. A spectrum analysis of the error signals further reveals the superiority of the proposed algorithm. We can see from Fig. 10, that compared to the standard DOB, the proposed algorithm had a much higher disturbance rejection band. Errors below 2000 Hz were greatly reduced due to the high cut-off frequency of Q-filter.

Finally, the magnitude responses from the input disturbance to the plant output are shown in Fig. 11. The response in the proposed DOB exhibits a much deeper magnitude drop in the middle frequency region, resulting in a larger disturbance rejection capacity. A small high frequency region gets slightly amplified, due to the *waterbed* effect that it is theoretically impossible for the closed loop transfer function to simultaneously have small magnitudes at all frequencies. However, since the low frequency disturbance dominates, overall the error is better attenuated.

V. CONCLUSION

This paper has presented a new method to expand the DOB disturbance rejection capacity. When low fre-

[2]The feedback controller in this case is the same PD controller cascaded with several notch filters.

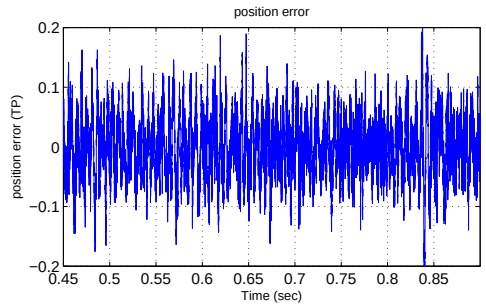

(a) applying the standard DOB: σ = 0.0518

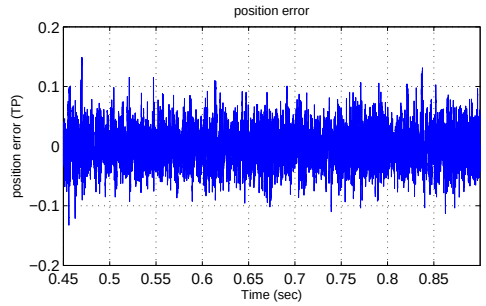

(b) applying the proposed DOB: σ = 0.0319

Fig. 9. Time traces of the tracking errors.

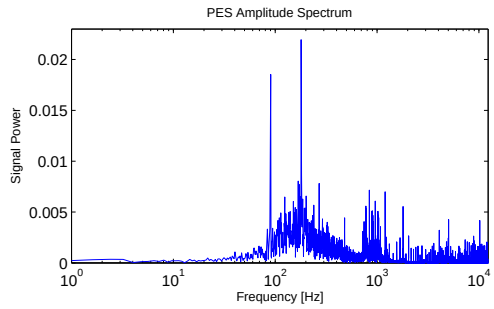

(a) applying the standard DOB

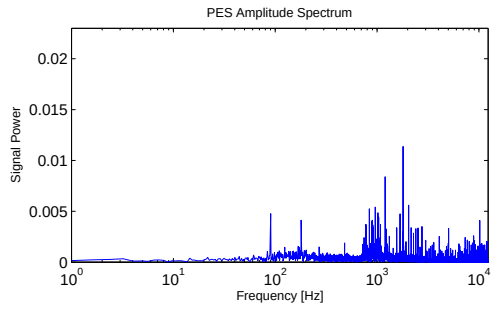

(b) applying the proposed DOB

Fig. 10. Frequency spectra of the tracking error.

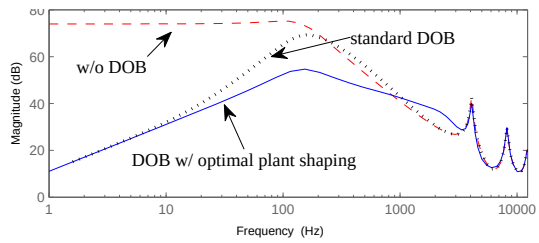

Fig. 11. Magnitude response from input disturbance to plant output.

quency disturbance dominates in a control system that has high frequency resonances, the proposed algorithm provides more freedom for designing the cut-off frequency of the Q-filter. Compared with the standard DOB, simulation showed significant reduction in the tracking error.

ACKNOWLEDGMENTS

This work was supported by the Computer Mechanics Laboratory (CML) in the Department of Mechanical Engineering, University of California at Berkeley.

References

[1] M. White, M. Tomizuka, and C. Smith, "Rejection of disk drive vibration and shock disturbances with a disturbance observer," in *Proc. 1999 American Control Conference*, vol. 6, 1999, pp. 4127–4131.

[2] J. Ishikawa and M. Tomizuka, "Pivot friction compensation using an accelerometer and a disturbance observer for hard disk drives," *IEEE/ASME Transactions on Mechatronics*, vol. 3, no. 3, pp. 194–201, 1998.

[3] M. White, M. Tomizuka, and C. Smith, "Improved track following in magnetic disk drives using a disturbance observer," *IEEE/ASME Transactions on Mechatronics*, vol. 5, no. 1, pp. 3–11, 2000.

[4] K. Yang, Y. Choi, and W. K. Chung, "On the tracking performance improvement of optical disk drive servo systems using error-based disturbance observer," *IEEE Transactions on Industrial Electronics*, vol. 52, no. 1, pp. 270–279, Feb. 2005.

[5] K. Tan, T. Lee, H. Dou, S. Chin, and S. Zhao, "Precision motion control with disturbance observer for pulsewidth-modulated-driven permanent-magnet linear motors," *IEEE Transactions on Magnetics*, vol. 39, no. 3 Part 2, pp. 1813–1818, 2003.

[6] S. Komada, M. Ishida, K. Ohnishi, and T. Hori, "Disturbance observer-based motion control of direct drive motors," *IEEE Transaction on Energy Conversion*, vol. 6, no. 3, pp. 553–559, 1991.

[7] C. Kempf and S. Kobayashi, "Disturbance observer and feedforward design for a high-speeddirect-drive positioning table," *IEEE Transactions on Control Systems Technology*, vol. 7, no. 5, pp. 513–526, 1999.

[8] C. Wang and M. Tomizuka, "Design of robustly stable disturbance observers based on closed loop consideration using h-infinity optimization and its applications to motion control systems," in *Proc. 2004 American Control Conference*, 2004, pp. 3764–3769.

[9] Y. Choi, K. Yang, W. Chung, H. Kim, and I. Suh, "On the robustness and performance of disturbance observers for second-order systems," *IEEE Transactions on Automatic Control*, vol. 48, no. 2, pp. 315–320, 2003.

[10] B. Kim and W. Chung, "Advanced disturbance observer design for mechanical positioning systems," *IEEE Transactions on Industrial Electronics*, vol. 50, no. 6, pp. 1207–1216, 2003.

[11] C. Kempf and S. Kobayashi, "Discrete-time disturbance observer design for systems with time delay," in *Proc. 1996 4th International Workshop on Advanced Motion Control*, vol. 1, Mar 1996, pp. 332–337 vol.1.

[12] T. Murakami and K. Ohnishi, "Advanced motion control in mechatronics-a tutorial," in *Proc. IEEE Workshop on Intelligent Motion Control*, vol. 1, 1990, pp. 9–17.

[13] M. Tomizuka, "Zero phase error tracking algorithm for digital control," *Journal of Dynamic Systems, Measurement, and Control*, vol. 109, no. 1, pp. 65–68, 1987.

[14] B. Baker and A. Moraru, "Servotrackwriter with improved positioning system," *IEEE Transactions on Magnetics*, vol. 33, no. 5, pp. 2623–2625, Sep 1997.

[15] M. Kobayashi, S. Nakagawa, T. Atsumi, and T. Yamaguchi, "High-bandwidth servo control designs for magnetic disk drives," in *Proc. 2001 IEEE/ASME International Conference on Advanced Intelligent Mechatronics*, vol. 2, 2001, p. 1124âĂŞ1129.

[16] M. Hirata, "Nss benchmark problem of hard disk drive system," http://mizugaki.iis.u-tokyo.ac.jp/nss/.